Dielectric Spectroscopy on Dilute Blends of Polyisoprene/Polybutadiene: Effects of Matrix Polybutadiene on the Dynamics of Probe Polyisoprene†

Keiichiro Adachi,* Takao Wada, Tatsuyoshi Kawamoto, and Tadao Kotaka*,‡

Department of Macromolecular Science, Osaka University, Toyonaka, Osaka 560, Japan

Received November 21, 1994; Revised Manuscript Received March 9, 1995®

ABSTRACT: Dielectric normal mode relaxation was studied on blends containing a small amount (~5 wt %) of probe *cis*-polyisoprenes (PI) in a series of polybutadienes (PB) of different molecular weights M_B. Since the PI chain has Stockmayer's type-A dipoles parallel to the chain contour, while PB chains do not, we can study global motion dynamics of the probe chain under various *entanglement* conditions between PI and PB chains. The dielectric normal-mode relaxation time τ of PI with molecular weight M_I followed a power law relation $\tau \propto M_I^{\alpha}$ with α varying from 2 to 3 depending on M_B: For $M_B < 3000$, $\alpha = 2.0 \pm 0.1$ in agreement with the Rouse model, while for $M_B > 20\,000$, $\alpha = 3.0$, conforming to the pure reptation model, and in the range $3000 < M_B < 12\,000$ α increased rather sharply with M_B. When τ was reduced to an isofriction state τ_ζ, the log τ_ζ *versus* log M_I plots for different M_B converged at $M_I = 1900$ (≅the entanglement spacing M_{eB} of bulk PB). The slope α of each log τ_ζ *versus* log M_I plot at constant M_I/M_B (>1) was larger than 3 and became 3.7 (observed for monodisperse PI melts) at $M_I/M_B \cong 2-3$. These findings were consistently interpreted with Graessley's constraint release model. The shape of the dielectric loss curves (reflecting the distribution of relaxation times) of the blends agreed rather well with the Rouse model when $M_I/M_B > 10$ and $M_B < M_{eB}$, but the loss curves became broader with decreasing M_I/M_B (or increasing $M_B > M_{eB}$) especially in the high-frequency tail, as usually observed in monodisperse PI melts.

Introduction

Dielectric spectroscopy is a powerful tool for studying molecular dynamics and conformational properties of polymers.[1-3] Especially when it is applied to Stockmayer's *type-A* chain,[1] defined as that having monomeric dipole moments aligned parallel to the chain contour, it provides information on slow dielectric response involving fluctuation and orientation of the end-to-end polarization vector of the chain (dielectric *normal mode* process).[1-3]

For a system composed of (monodisperse) type-A chains of the moment $\mathbf{P}(t)$ ($=\mu\mathbf{R}(t)$ with $\mathbf{R}(t)$ being the end-to-end vector at time t and μ, the dipole moment per unit contour length of the chain), the complex dielectric constant ϵ^* at low frequency can be expressed with the autocorrelation $\langle\mathbf{R}(t)\cdot\mathbf{R}(0)\rangle$ of the end-to-end vector of the individual type-A chain.[1-3] Even if the polymer has *type-B* dipoles as well (that are the components *perpendicular* to the chain contour and thus *uncorrelated* with $\mathbf{R}(t)$), the dielectric response from the type-A dipoles can be easily distinguished from the high-frequency *segmental modes* due to the type-B dipoles.[2,3] For the blends of two monodisperse type-A chains their response can also be easily separated, if their molecular weights are sufficiently apart. For the blends of type-A chains with *miscible* type-B chains (of any molecular weights), resolution of the normal modes is much easier. Dielectric spectroscopy on a system involving a probe (monodisperse) type-A chain is in fact the only method available to directly determine $\langle\mathbf{R}(t)\cdot\mathbf{R}(0)\rangle$ of the probe chain almost regardless of its environment. In other methods for examining probe chain dynamics such as, for example, neutron scattering, the labeling of the probes with deuterium is indispensable since it might alter the thermodynamics of the system. However, in dielectric spectroscopy using a monodisperse type-A polymer as a probe, the labeling is totally unnecessary.

As we have repeatedly pointed out, high *cis*-content polyisoprene (PI) is an excellent dielectric probe possessing both type-A and type-B dipoles, while polybutadiene (PB) of a certain microstructure is a type-B polymer *miscible* with PI.[2,3] Thus, applying dielectric spectroscopy, we were able to extract the probe chain dynamics to test currently proposed molecular theories of polymer melt dynamics.[4] The systems examined included, besides monodisperse PI solutions and melts,[2] PI/PI blends,[5] free PI chains in PB networks,[6] PI/PB blends,[7] and a ternary system involving PI in semidilute PB solutions.[8] The versatility of the systems allowed examination of the models appropriate for both *unentangled* and *entangled* polymers.

Background

For unentangled systems we consider the *Rouse* model, while for entangled systems we first consider the original *tube* model.[4] Interestingly, both models predict the relaxation mode distribution or the distribution of relaxation times of the same form:

$$\langle\mathbf{R}(t)\cdot\mathbf{R}(0)\rangle = (8\langle R^2\rangle/\pi^2)\sum_{p:\text{odd}}(1/p^2)\exp(-t/\tau_p) \quad (1)$$

Here τ_p ($=\tau_1/p^2$) is the relaxation time of the pth *normal* mode, and τ_1, the longest relaxation time that is different for the models.[4] This mode distribution leads to the dielectric loss ϵ'' *versus* angular frequency ω curve of the form

† An extended abstract was published in: *Polym. Prepr. (Am. Chem. Soc., Div. Polym. Chem.)* **1994,** *35* (1), 127.

‡ Present address: Toyota Technological Institute, Tempaku, Nagoya 468, Japan.

® Abstract published in *Advance ACS Abstracts,* April 15, 1995.

0024-9297/95/2228-3588$09.00/0

$$\frac{\epsilon''}{\Delta\epsilon} = \frac{8}{\pi^2} \sum_{p:\text{odd}} \frac{\omega\tau_p}{p^2(1+\omega^2\tau_p^2)} \quad (2)$$

Note that in eqs 3 and 4 only *odd-numbered* modes ($p = 1, 3, 5, ...$) with the characteristic time $\tau_p = \tau_1/p^2$ and the intensity proportional to p^{-2} are important.[1] Both the Rouse and tube models predict the dielectric loss curve of the same form, in which $\epsilon'' \propto \omega$ in the low-ω tail, but $\epsilon'' \propto \omega^{-1/2}$ in the high-ω tail.

The dielectric relaxation strength $\Delta\epsilon$ for the normal modes of a type-A chain of the mean square end-to-end length $\langle R^2\rangle$ is given by[1,2]

$$\Delta\epsilon = 4\pi c N_A \mu^2 \langle R^2\rangle F/(3Mk_BT) \quad (3)$$

with c being the mass concentration (or the density for the bulk), N_A, the Avogadro constant, F, the ratio of the internal to the external field (that can be taken as 1 for the normal modes),[2,3] M, the molecular weight (for a polydisperse type-A polymer this should be the weight-average value), and k_BT, the thermal denergy.

In these two models, however, the expression of the longest relaxation time τ_1 is different.[2-4] The Rouse model[9] predicts τ_1, often referred to as the Rouse relaxation time, τ_R, for unentangled flexible-linear chains as

$$\tau_1 (\equiv\tau_R) = \zeta N^2 b^2/(3\pi^2 k_BT) \propto \zeta_0 M^2 \quad (4)$$

where ζ is the friction coefficient of each bead connected with N identical segments of the mean square length b^2. Note that $N \propto M = ZM_0$, $\langle R^2\rangle = Nb^2$, and $\zeta N = \zeta_0 Z$ with ζ_0 being the monomeric friction coefficient, Z, the degree of polymerization, and M_0, the molar mass of the monomeric unit.

On the other hand, the tube model proposed by de Gennes[10] and by Doi and Edwards[4,11] predicts τ_1 ($\equiv\tau_d$), referred to as the *tube disengagement* time or the *reptation* time, for entangled linear chains as

$$\tau_1 (\equiv\tau_d) = 3\tau_R(M/M_e) \propto \zeta_0 M^3 \quad (5)$$

with M_e being the molecular weight between entanglements.[4,12-14]

We usually define (dielectric) *nominal* relaxation time τ as $\tau = 1/(2\pi f_m)$ from the loss maximum frequency f_m at which the observed ϵ'' peak for the normal modes becomes maximum. As seen in eqs 1 and 2 for the two models, the contribution of the fundamental mode ($p = 1$) is as large as 81% of the observed peak and the nominal relaxation time $\tau \cong 0.97\tau_1$.

Experimental results of dielectric as well as viscoelastic spectroscopies[12-14] reported so far on monodisperse polymers[2,3] show that for unentangled chains with M less than the characteristic molecular weight M_c ($\cong 2M_e$), τ exhibits M^2 dependence in agreement with the Rouse model. However, for entangled chains with $M \geq M_c$, τ exhibits $M^{3.5}$ dependence, and the M^3-dependent relaxation times were never found for monodisperse bulk systems.[2,3,12-14] This discrepancy was believed to be due to the oversimplification of the original tube model.[10,11]

The tube model assumes a single process of relaxation: each polymer molecule, constrained by *uncrossability* of surrounding molecules, moves and changes its conformation only through diffusion along the contour (*reptation* in a tube).[4,14] Later proposed were two other mechanisms, *contour length fluctuation*[15] and *constraint release*,[13,16,17] which contribute to increasing the diffusion rate and thus decrease the relaxation time. Constraint release was first proposed by Klein[16] based on an idea of *tube renewal*: The probe molecule can also relax through the motion of the tube, because the surrounding tube-forming molecules as well are mobile and eventually diffuse away. The constraint release model was developed by Graessley[13] and further by Watanabe and Tirrell.[17]

We were able to test these mechanisms *via* dielectric spectroscopy on a trace amount of (monodisperse) PI chains used as a probe in a matrix with extremely *high-molecular-weight* PI chains or trapped in loosely cross-linked PB networks.[5,6] In these studies[2,3] we observed M^3-dependent relaxation times for the probe PI chains. These findings ruled out contour length fluctuation and suggested the constraint release mechanism is prevailing in the relaxation of monodisperse melts, especially near the crossover from unentangled to entangled behavior.

For elucidating the detailed features of polymer melt dynamics, we conducted dielectric spectroscopy on a series of *dilute* blends of probe PI chains with molecular weight M_I in matrix PB chains with M_B widely varying through its M_c. Here the term "*dilute* blends" implies that the probe chains *do not* entangle among themselves but may or may not *entangle* with the matrix chains.

Table 1. Characteristics of PI and PB Samples

code	$10^{-3}M_w$	M_w/M_n	code	$10^{-3}M_w$	M_w/M_n
		cis-Polyisoprenes (PI)[a]			
PI-0.8	0.79		PI-09	9.49	1.07
PI-01	1.04	1.10	PI-13	12.9	
PI-02	1.55	1.11	PI-27	27.0	
PI-03	2.64	1.09	PI-48	47.9	1.05
PI-04	4.84	1.07	PI-86	86.0	
PI-05	5.37	1.05	PI-140	140	1.05
PI-06	5.80	1.08			
		Polybutadienes (PB)			
PB-02	2.0	1.03	PB-20	20.0	1.04
PB-03[a]	2.5	1.03	PB-36	36	1.04
PB-05[a]	5.1	1.04	PB-45	45	1.05
PB-07	7.2	1.04			
PB-08	7.9	1.04	cPB-202[b]	202	2.11
PB-11	10.7				

[a] Microstructures of these samples are given in Table 2. [b] A commercial polybutadiene (Firestone, Diene 35 NF).

Experimental Section

Materials. Previously, we confirmed that *cis*-polyisoprenes (PI) and anionically polymerized polybutadiene (PB: $M \cong 5 \times 10^4$) of a particular microstructure (*e.g.*, 37% *cis*; 55% *trans*; 8% vinyl) are miscible even at a composition as much as 50/50 by weight.[6,18] We prepared narrow molecular-weight-distribution (MWD) samples of PI and PB *via* anionic polymerization in heptane, as reported previously.[6-8] We also used an anionically-polymerized but a broad MWD commercial PB sample (Firestone Diene 35NF, coded as cPB-202) as a matrix component. The weight-average molecular weight M_w and the polydispersity index M_w/M_n of these samples were determined on a gel permeation chromatograph (Tosoh Model HLC-801A) with a low-angle laser light scattering detector (Tosoh LS-8000). The microstructure was determined by ^{13}C NMR: For PB samples the assignment reported by Clague *et al.*[19] was employed. The sample characteristics are listed in Tables 1 and 2. The codes indicate the values of M_w in kilograms per mole.

The blends were prepared as follows. In each case, PI and PB samples of the weight-average molecular weights M_I and M_B were taken at the ratio of 5/95 by weight, respectively, and dissolved in *n*-hexane to make an approximately 5% homogeneous solution. Then the solvent was thoroughly evaporated

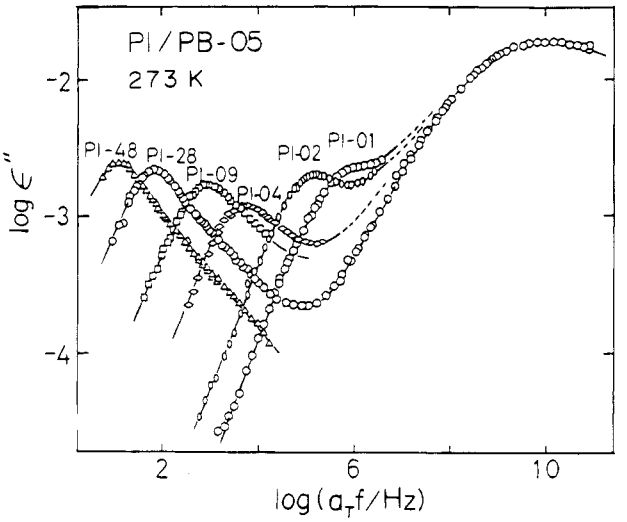

Figure 1. Master curves of log ϵ'' *versus* log $a_T f$ for PI/PB-05 blends at 273 K. The PI content is approximately 5 wt % for all the blends.

Table 2. Polydiene Microstructure (%)

code	*cis*	*trans*	3,4-vinyl
a: PIs av	83	13.5	3.5
b: PB-03	38	55	7
c: PB-05	40	49	11
d: cPB-202	37	55	8

and the blend was dried under a vacuum of 0.01 Torr for 50 h at about 45 °C. For the PI-140/PB-03 blend we also prepared a 3/97 blend to see if the blends are dilute enough.

Methods. The dielectric loss factor ϵ'' was measured with a transformer capacitance bridge (General Radio, Model 1615A) in the range of frequency f from 100 Hz to 18 kHz according to our laboratory routine.[4-8] To cover a wide range of time scale, we constructed master curves of ϵ'' *versus* the reduced frequency $a_T f$ by taking the reference temperature T_S as 273 K.

Results and Discussion

1. Frequency Dependence of Dielectric Loss Factor ϵ''. Figures 1 and 2 show representative ϵ'' *versus* $a_T f$ master curves at 273 K for PI/PB-05 and PI/cPB-202, respectively, where a_T is the shift factor. The loss peaks seen in the audio-frequency range of 10 Hz to 100 kHz are due to the normal modes of the PI probes, and the (nearly M_I- and M_B-independent) high-frequency peak around 10 GHz is due to the segmental modes of both PI and PB.

The ϵ'' master curves of the blends show clear loss maxima due to the normal mode when M_I is higher than 2×10^3. However, for the blends with $M_I < 2 \times 10^3$, the contributions from the normal and segmental modes begin to overlap.

Thus accurate determination of the loss maximum frequency f_m requires resolution of the peaks. To do this, we assumed for all PI/PB-05 blends that the ϵ'' values (in the range $f > 100$ kHz) due to the segmental mode are the same as those of PI-81/PB-05 for which the normal mode peak locates around f_m of 10 Hz, and hence the ϵ'' curve in the range $f > 100$ kHz can be regarded as due totally to the segmental mode. On the other hand, for PI/cPB-202 we determined the contribution of the segmental mode as 95% of the ϵ'' values of pure cPB-202. Either one of these two methods was applied to other blends.

2. Shift Factor. Figure 3 shows shift factor a_T *versus* T plots used for superposition of the ϵ'' curves at

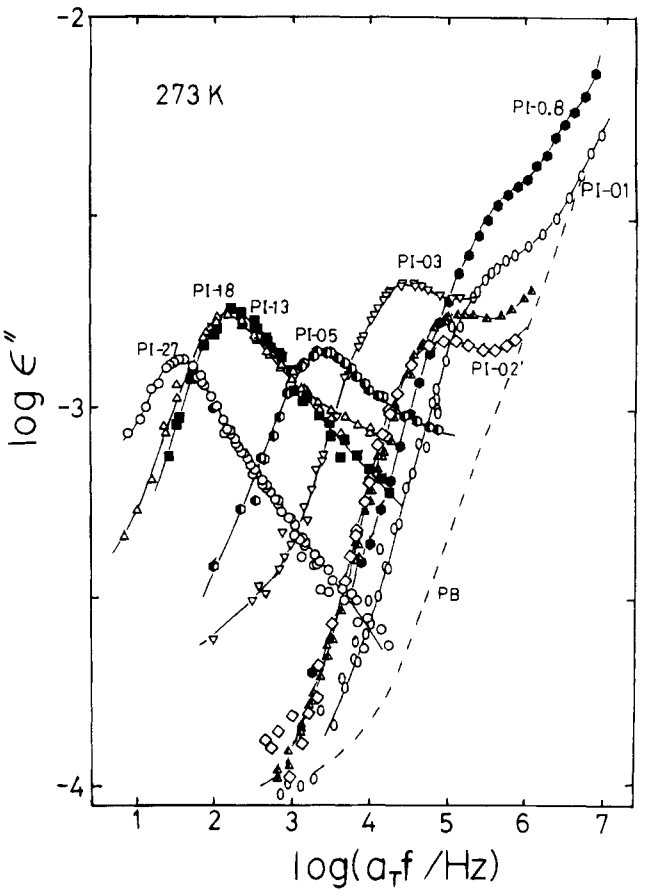

Figure 2. Master curves of log ϵ'' *versus* log $a_T f$ for PI/cPB-202 blends at 273 K. The PI content is approximately 5 wt % for all the blends.

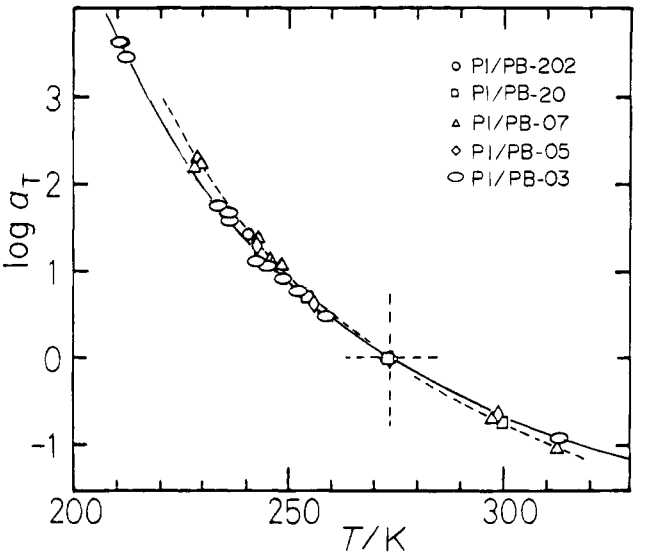

Figure 3. Temperature dependence of the shift factor a_T for PI/PB blends and PB melts. The smoothed solid curve is for PI/PB-03 blends, and the dashed curve, for other blends and PB melts with $M_B > 5000$.

$T_S = 273$ K. We see that the plots for PI/PB-03 (the solid line) and PI/PB-02 (although not shown here) slightly deviate from that for other blends (the dashed curve). This deviation implies that the friction factors ζ for the probe PI chain in PB-02 and PB-03 are smaller than those in other matrices with $M_B > 5 \times 10^3$. The Williams–Landel–Ferry constants[12,20] for the former blends were determined to be $C_1 = 3.95$ and $C_2 = 130$ K, whereas those for the latter were $C_1 = 4.6 \pm 0.3$ and

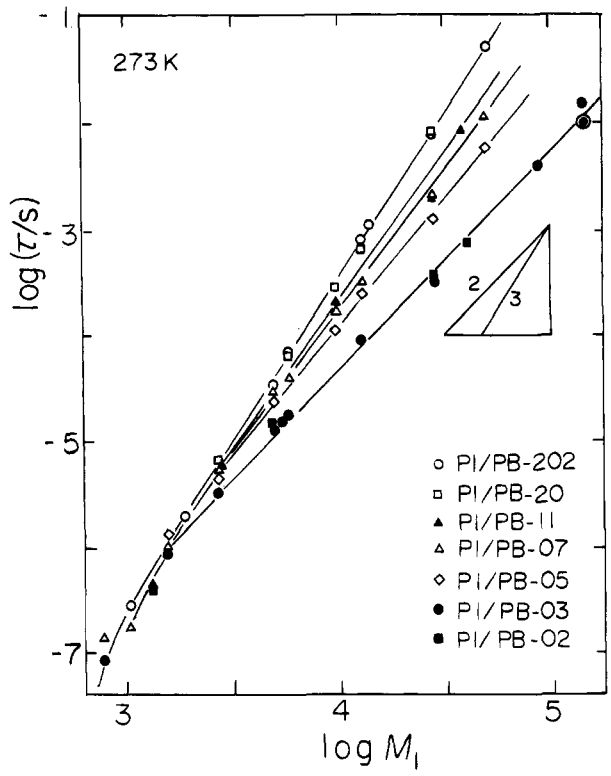

Figure 4. Normal mode relaxation time log τ *versus* log(molecular weight, M_I) for PI probes in PI/PB blends at T = 273 K. The double circle at log M_I = 5.2 represents τ for a blend PI-140/PB-03 containing 3% PI-140.

C_2 = 138 ± 7 K. These values of a_T agree with those reported by Colby *et al.*[21] for reducing the data of viscoelastic properties of PB (*not* those of PI). The fact reflects that the PB matrices overwhelm the melt dynamics of the PI/PB blends studied here. Later we will use these a_T data to reduce the relaxation time data to those for an *isofriction* state.

3. Relaxation Times of the Probe PI Chain in the PB Matrix. Nominal Relaxation Times. As usual we determined the nominal (dielectric) relaxation time τ of PI as $\tau = 1/(2\pi f_m)$ from the loss maximum frequency f_m for the normal modes. However, the observed peaks were almost always broader than the theoretical peak, especially in the high-f tail where $\epsilon'' \propto f^{-n}$ with $n \cong 0.33-0.3$ (instead of 0.5 for either the Rouse or the tube model). Nevertheless we may assume $\tau \cong \tau_1$ for an observed peak with $\epsilon'' \propto f$ in the low-f tail, because such a loss peak still essentially reflects the fundamental (p = 1) mode if the probe PI chain has a narrow MWD (*e.g.*, with $M_w/M_n < 1.1$).[2,3]

Figure 4 shows the dependence of thus determined τ (uncorrected for ζ) on M_I for the PI/PB blends examined here. We see that the PI/PB-02 and PI/PB-03 the slope α of the log τ *versus* log M_I plots is 2.0 ± 0.1, conforming to the Rouse model, eq 3. In contrast, α is 3.0 ± 0.1 for PI/cPB-202 and for those blends with $M_B > 20 \times 10^3$. The power of 3 agrees well with the pure reptation model, eq 4. These M^3-dependent relaxation times were never found in other experiments such as viscoelastic spectroscopy.[11-14] Interestingly, when M_B is increased in the range between 5×10^3 (PB-05) and 20×10^3 (PB-20), the log τ *versus* log M_I plots are nearly straight lines with the slope α varying continuously from 2 (the Rouse behavior) to 3 (pure reptation).

Effect of Probe Concentration. In order to examine more closely the dependence of τ on M_I and M_B for the PI/PB blends and compare with the current theories, we should collect the τ data preferably at infinite dilution or at least below the *overlapping* concentration c^* of the probe chains defined as $c^* = 3(6)^{3/2}M/(4\pi N_A\langle R^2\rangle^{3/2})$. To check this point, we estimated c^* for the probe PI chains in the present blends. The representative values of c^* are 0.05 for PI-27, 0.04 for PI-48, and 0.023 for PI-140. Thus the 5 wt % blends containing PI with M < 27 000 may be regarded as *dilute* but those of PI-48 and PI-140 may be in the semidilute regime. The entanglement spacing for PI probe chains, however, can be as large as 100 000 for the 5 wt % blends and 160 000 for the 3 wt % blends. Then PI-140 chains in the 3 wt % blend and PI-48 in the 5 wt % blend are still in the unentangled state but PI-140 chains in the 5 wt % blend may be in the crossover region of the entangled and unentangled states. In fact in Figure 4, we see that the 3 wt % PI-140/PB-03 blend appears to exhibit M^2-dependent relaxation time but the 5 wt % blend deviates from the Rouse behavior.

Effect of Excluded Volumes. Another factor to be considered is the effect of excluded volumes in the dilute blends. In our previous paper[5] on the dielectric normal mode relaxation in the dilute binary blends of the high-molecular-weight (HMW) PI probe in the low-molecular-weight (LMW) PI matrix, we reported the excluded volume expansion of the HMW probe chains in the LMW matrix chains when $M_{HMW} > M_{LMW}^2$, as predicted by Flory.[22] In the present systems there is also a possibility that the HMW-PI chains assume an expanded conformation in the LMW-PB matrices. We estimated, by using eq 3, the mean-square expansion factor $\langle R^2\rangle/\langle R^2\rangle_0$ for the mean-square end-to-end distance, where the suffix o indicates the unperturbed value determined for pure PI melt with M the same as the probe PI chain. The expansion factors thus estimated can be regarded to be unity within the error of ±0.1, except for the PI-140/PB-03 system for which the value is roughly 1.2. The correction due to this expansion was trivial. The LMW-PI chains are an athermal solvent toward HMW-PI chains, but the LMW-PB chains, although miscible with PI chains, are certainly a poorer solvent. Thus we may conclude that the excluded volume effect is unimportant in these dilute PI/PB blends.

Isofriction State Relaxation Times τ_ζ. The most important correction to be made to interpret the relaxation time data is the correction for the differences in ζ for the matrix PB chains and the probe PI chains of the blends. Such a correction was made as follows.

(i) Correction of ζ for PB. From the shift factor a_T data (Figure 3), we see that the effective friction coefficient ζ_{LMW} of PI probes in the LMW matrices, PB-02 and PB-03, is lower than ζ_{HMW} in the HMW matrices with $M_B > 5 \times 10^3$. We estimated the difference $\zeta_{HMW} - \zeta_{LMW}$ by starting from the universal WLF equation of the form

$$\log[\zeta(T)/\zeta(T_g)] = -C_1'(T - T_g)/(C_2' + T - T_g) \quad (6)$$

where the glass transition temperature of the matrix T_g is dependent on M_B and C_1' (≡17.44) and C_2' (≡51.6) are the universal WLF constants independent of M_B.[12,20] Here we assume $\zeta(T_g)$ is a constant independent of M_B, if compared at the respective M_B-dependent T_g, and the difference $\zeta_{HMW} - \zeta_{LMW}$ can be ascribed to the difference in T_g, $\Delta T_g = T_g^{HMW} - T_g^{LMW}$, of the matrix PBs. Then from eq 6 with the observed values of T_g's for the present systems we obtain

$$\log \zeta_{HMW} - \log \zeta_{LMW} = C_1'C_2'\Delta T_g/(C_2' + T - T_g^{HMW})^2 = 0.20 \quad (7)$$

where the difference ΔT_g was neglected in the denominator.

The value of 0.20 in eq 7 for the present blends was determined as follows: First ΔT_g was determined to be 6 K from the horizontal shift needed in Figure 3 to superpose the log a_T curve for PI/PB-03 (the solid line) on that for the other blends with $M_B > 5 \times 10^3$ (the dashed line). Then T_g^{HMW} was estimated to be 161 K from $T_g^{HMW} = T_s + 51.6 - (C_1'C_2'C_2/C_1)^{0.5}$ where $T_s = 273$ K and C_1 and C_2 are given for the high-molecular-weight matrix blends (*cf.* Figure 3).[12]

(ii) Correction of ζ Due to PI. For the dilute PI probe in short PB matrix chains, the Rouse theory predicts τ_1 ($\equiv\tau_R$) $\propto \zeta_0 M_I^2$. This is the case for the two blends with PB-02 and PB-03 (*cf.* Figure 4). However, by closely examining Figure 4, we notice that data points for the probes with $M_I < 1.6 \times 10^3$ (PI-02) ($<M_e$) always deviate downward from the Rouse behavior, regardless of M_B. This deviation was usually observed for short monodisperse melts with $M < M_e$ and is interpreted as due to the change in ζ_0 for the short probes resulting from the chain ends around which extra free volumes can be created even in a high-molecular-weight matrix. However, at the moment there are no theories available to express such a local free volume effect on the glass transition. We thus simply assume the isofriction state relaxation time τ_ζ for the short probe chains will appear on the extrapolation of the Rouse line, as shown with the dashed line in Figure 5.

On the basis of these considerations we reduced τ for PI/PB-02 and PI/PB-03 blends to that of the HMW blends and constructed log τ_ζ *versus* log M_I plots at the isofriction state in Figure 5 for the PI probes with $M_I > 5 \times 10^3$. In Figure 5 we see that the isofriction state plots converge at $M_I = 1900$ (that is nearly equal to M_e for bulk PB and much smaller than $M_e \cong 5000$ for bulk PI).[12] Thus an empirical equation for the log τ_ζ *versus* log M_I plots can be

$$\log \tau_\zeta = \alpha \log(M_I/1900) - 5.63 \qquad \text{for } M_I > 1900 \quad (8)$$

where the slope α varies with M_B as $\alpha = 2.0$ for PI/PB-02 and PI/PB-03, 2.41 for PI/PB-05, 2.58 for PI/PB-07, 2.77 for PI/PB-11, 2.95 for PI/PB-20 and 3.0 for PI/PB-202, as shown in Figures 5 and 6. We found the α *versus* M_B relation best represented by

$$\alpha = 3 - \exp[-(M_B/8500)^{1.5}] \quad (9)$$

This equation is just an empirical equation, and another functional form may be used to better represent the M_B dependence of α. Anyway, combining eqs 8 and 9, we can express τ_ζ as a function of M_I and M_B.

4. Competition of the Reptation and Constraint Release Mechanisms. We have seen that the M_I dependence of τ_ζ ($\propto M_I^\alpha$) of the dilute PI/PB blends changes, depending on M_B, with α varying from 2 (for LMW matrices) up to 3 (for HMW matrices). These results obviously imply that in the former blends the matrix chains surrounding a probe chain can be regarded as solvent molecules in which the probe chain behaves as an unentangled Rouse chain. On the contrary, in the latter blends the matrix chains hardly move and thus can be regarded as a fixed tube imposing a severe constraint on the probe chain that can thus relax only by diffusion along the tube contour, *i.e.*, by *reptation*.

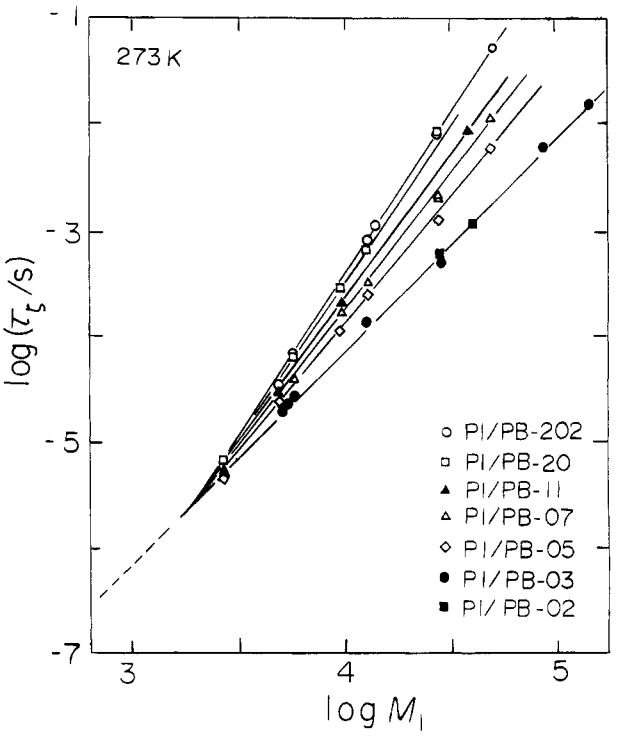

Figure 5. Relaxation time τ_ζ reduced to the *isofriction* state corresponding to high-molecular-weight PB matrices at 273 K.

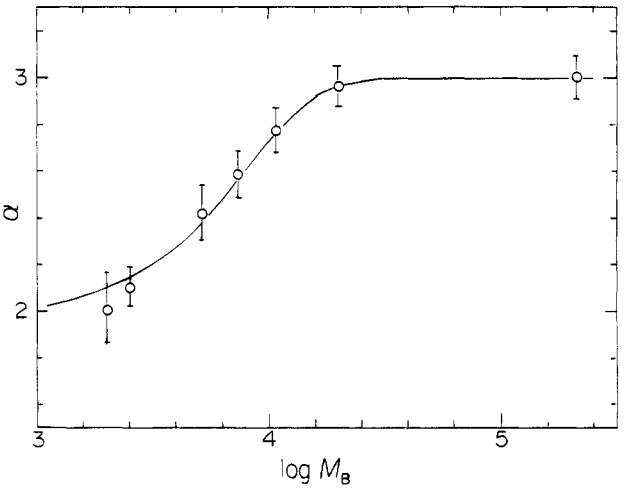

Figure 6. Matrix PB molecular weight M_B dependence of the index α in $\tau_\zeta \propto M_I^\alpha$.

Then a question arises why (monodisperse) HMW melts exhibit an $\alpha = 3.5$ power rather than 3. Since the possibility of *contour length fluctuation*[15] may be ruled out by the fact that the HMW matrix blends exhibit M_I^3-dependent relaxation times, the difference in α is attributable to the difference in the environment of the probe chain: in a monodisperse melt the probe chain is surrounded by the same chains that are mobile at a comparable rate and thus can be regarded as a deformable tube (constraint release). The probe chain can relax *via* a balance between *reptation* and the *constraint release* mechanism[13,16,17] taking place simultaneously.

(i) Graessley's Constraint Release Model. In this context it is interesting to examine the details of the *constraint release* model of Graessley.[13] Consider a dilute blend in which a probe (guest) chain with M_g moves through surrounding matrix chains with M_m. (For the present blends they are M_I and M_B, respectively.) In such a melt, local portions of a tube confining the probe chain move *via* successive local jumps as the surrounding matrix chains diffuse away. The frequency of such random local jumps is proportional to the mobility of the surrounding chains and hence dependent on their molecular weight M_m. Due to such random local jumps the tube itself behaves like a Rouse chain, as suggested by Verdier and Stockmayer.[23] The constraint release time τ_{cr} was then given by Graessley as[13]

$$\tau_{cr} = (2\Lambda/\pi^2)(N/N_e)^2\tau_{d(m)} \quad (10)$$

where Λ is a constant related to another parameter called the *gate* number z for the local jumps (*i.e.*, an average number of gates at which such jumps can take place along the chain between entanglements, N/N_e ($\equiv M/M_e$) is the number of entanglements of the probe chain, and $\tau_{d(m)}$ is the reptation time (eq 5) of the matrix chain. The observed relaxation time $\tau_{(g)}$ of the probe chain is now determined by $\tau_{d(g)}$ and τ_{cr} as

$$1/\tau_{(g)} = 1/\tau_{d(g)} + 1/\tau_{cr} \quad (11)$$

From eqs 5, 10, and 11, we obtain $\tau_{(g)}$ as

$$\tau_{(g)} = \frac{\tau_{R(e)}\Lambda}{M_e^3\pi^2}\frac{M_g^2}{(M_e/M_m)^2 + (\Lambda/\pi^2)(M_m/M_g)} \quad (12)$$

where $\tau_{R(e)}$ is the Rouse relaxation time of the matrix chain with $M = M_e$. Note that for LMW matrix blends in which we can assume M_e/M_m approaches a constant of the order of 1 and $M_m/M_g \to 0$, then $\tau_{(g)} \propto M_g^2$, while for HMW matrix blends in which $M_e/M_m \to 0$ and M_m/M_g approaches a constant larger than 1, $\tau_{(g)} \propto M_g^3$.

A more meticulous treatment of the constraint release mechanism was suggested by Watanabe and Tirrell.[17] However, as long as the longest relaxation time is concerned, the Graessley theory is probably good enough to explain the features of the observed dependence of τ on M_g and M_m.

(ii) Comparison with the Experiments. Now we apply eq 12 to interpret the τ data of our dilute PI/PB blends. The Graessley model considers relaxation of a probe chain mixed with matrix chains of the chemically same kind. Thus the assignment of the parameters is straightforward. But our dilute blends are composed of a probe PI chain moving through an entanglement network of matrix PB chains. The entanglement spacing M_e should be that of PB but *not* of PI. Then, assuming the parameter $\Lambda = 0.114$ (corresponding to the gate number $z = 4$) and $M_e = 1900$ (of PB melts), we calculated $\tau_{(g)}$ from eq 12 as plotted in Figure 7. We see that eq 12 fairly well reproduces the features of Figure 5, although each calculated log $\tau_{(g)}$ versus log M_g curve does not strictly obey the power law dependence with a constant α ($2 \le \alpha \le 3$) but asymptotically approaches the Rouse behavior with $\alpha = 2$, as M_g is increased far beyond M_m. A long probe chain of $M_g \gg M_m$ might regard the surrounding matrix chains simply as solvent molecules irrespective of M_m. In the present study, however, we did not cover the range of M_I high enough to see such asymptotic behavior.

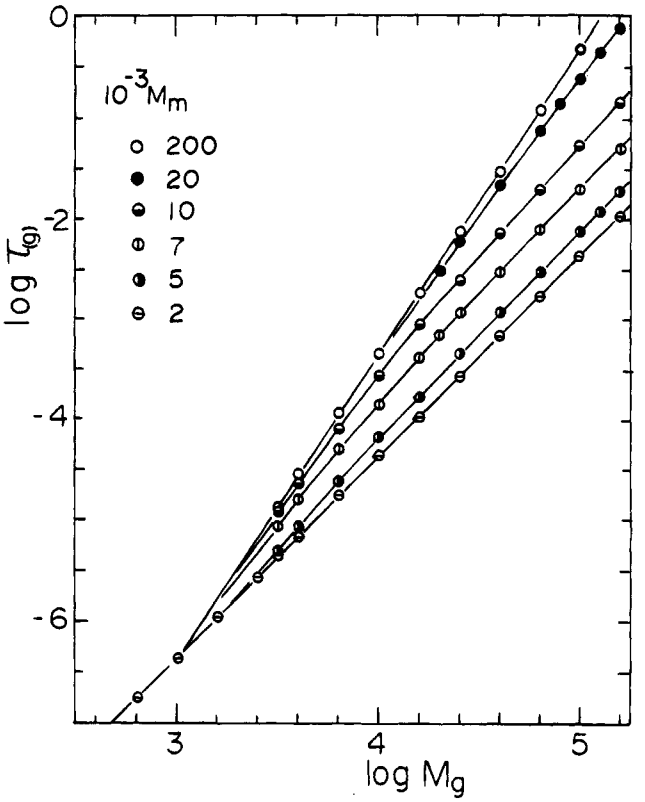

Figure 7. Double logarithmic plots of $\tau_{(g)}$ *versus* M_g calculated with eqs 10 and 11 proposed by Graessley.[13] The parameter Λ was taken to be 0.114 with the gate number $z = 4$. The entanglement spacing M_e was taken to be 1900 corresponding to the PB matrix used here.

5. Relaxation Times at a Constant Ratio of M_I/M_B. Now we return to the problem of how reptation and constraint release mechanisms are competing in the relaxation of monodisperse melts. In order to examine the features of such behavior, it should be worthwhile to examine the M_I dependence of τ_ξ at constant ratios of M_I/M_B. Figure 8 shows plots of log τ_ξ *versus* log M_I at $M_I/M_B = 1-4$ calculated with eqs 8 and 9. Although the plots do not exactly follow straight lines, we draw reasonably good best fit lines with the slope α varying from 2 to 4 except in the narrow region of M_I close to M_c ($\cong 10^4$ for monodisperse PI melts), where $\alpha > 3$.

We also see that the 3.7 power dependence for monodisperse PI melts[2] is seen in our PI/PB blends with $M_I/M_B \cong 2-3$ at around M_c. A PB chain with M_B is equivalent to a PI chain with $M_I \cong 2-3$ times M_B in the entanglement coupling behavior. This is an interesting result in view of the fact that M_e of PI is 5000 while that of PB is 1900, and thus $M_e(PI)/M_e(PB) \cong 2.5$.[12,13] In our previous study on PI–PB block copolymers, we also obtained a similar conclusion: a PB block segment with M_B is equivalent to a PI segment with $M_I \cong 2M_B$ in their entangled regime.[24]

Then the next question to be asked is in a monodisperse melt up to how high M the competition between reptation and constraint release can go? In a monodisperse melt the constraint release for an arbitrary probe chain takes place as a result of reptation of many surrounding chains identical to the probe chain. The constraint release time is thus expected to be $\tau_{cr} \propto M^5$. Then τ_{cr} could be far longer than its own reptation time $\tau_d \propto M^3$ in the limit of extremely high M. In such a

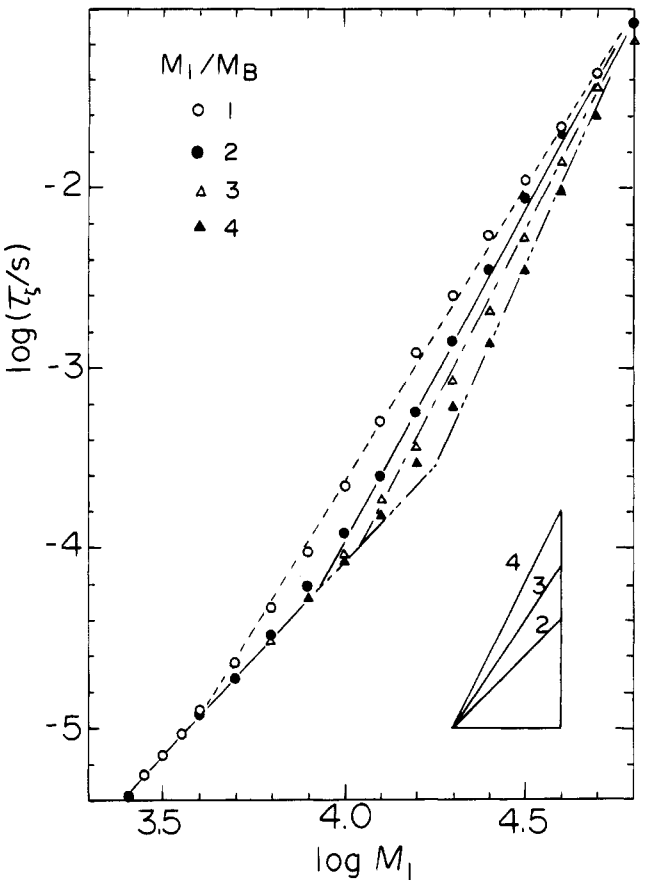

Figure 8. Double logarithmic plots of τ_ζ *versus* M_I at constant M_I/M_B from 1 to 4 calculated with eqs 8 and 9.

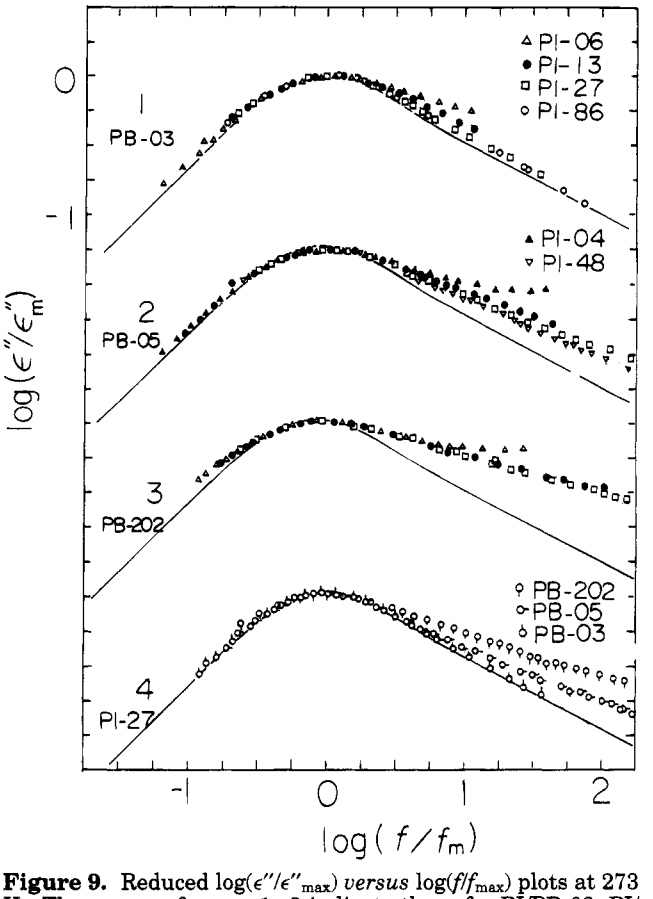

Figure 9. Reduced $\log(\epsilon''/\epsilon''_{max})$ *versus* $\log(f/f_{max})$ plots at 273 K. The curves of group 1–3 indicate those for PI/PB-03, PI/PB-05, and PI/cPB-202, respectively. The curves of group 4 indicate those for PI-27 in PB-03, PB-05, and cPB-202. The solid curve in each group represents the loss curve from the Rouse/tube theory.

case reptation might overwhelm constraint release. In fact, for extremely high-molecular-weight (monodisperse) PB melts, Graessley presented a piece of evidence for the M^3-dependent relaxation times (precisely M^3-dependent zero shear viscosities) as an asymptotic behavior in the range of M as high as $M > 150M_e$.[21] However, the above argument as well as the said experimental evidence itself is still to be tested carefully. Obviously, it is not necessary for all the surrounding chains to *reptate away* completely before constraint release to take place.

6. Relaxation Mode Distribution. Finally, we turn our attention to the problem of relaxation mode distribution. In the preceding sections we see that, as long as the molecular weight dependence of τ is concerned, the Rouse model and the tube model combined with constraint release consistently explain the behavior of dilute PI/PB blends as well as monodisperse homopolymer melts. As to the relaxation mode distribution, we see from eqs 1 and 2 that both the Rouse and reptation theories predict the same distribution or the dielectric loss curve of the same form: in the log ϵ'' *versus* log f curve, $\epsilon'' \propto f$ in the low-f tail, but $\epsilon'' \propto f^{-1/2}$ in the high-f tail.

We found that only very dilute PI solutions conform to the Rouse model-type distribution.[8] As a matter of fact, the Zimm model[9] with preaveraged hydrodynamic interactions among the beads is a better approximation for dilute solutions: The Zimm theory predicts $\tau_1 \propto M^{1.5}$ but almost the same mode distribution as the Rouse model.[1-4,9]

However, both the Rouse and tube theories are still unsatisfactory for explaining the mode distribution of concentrated solutions as well as unentangled and entangled melts. In fact in PI solutions with increasing concentration beyond the overlapping concentration C^* (roughly 10 times below the entanglement concentration C_e), we found the shape of the $\log(\epsilon''/\epsilon_{max}'')$ *versus* $\log(f/f_{max})$ curve became broader than the Rouse curve, especially in the high-f tail where $\epsilon'' \propto f^{-n}$ with $n \cong 0.33-0.3$.[2,3,8] Here ϵ_{max}'' is the value of ϵ'' at f_{max}. This broadening of the loss curve was also seen for monodisperse PI melts even with $M < M_e$ (although separation of the normal and segmental mode peaks becomes more and more difficult for such low-M melts).[2,3,8] The broadening of the loss curve appears to be induced just by the overlapping of the chains and is *not* due to the onset of entanglements. The situation is quite different in the viscoelastic spectroscopy data: The G′ curve of a monodisperse melt, for example, begins to exhibit a *rubbery plateau* as soon as M exceeds M_e, *i.e.*, the onset of entanglements.[12,13]

The similar broadening of the loss curves was seen also in the present dilute blends. Figure 9 shows the reduced loss curves for four series of the blends. Groups 1–3 represent PI/PB-03, PI/PB-05, and PI/cPB-202 blends, respectively, for which the probe M_I was changed as indicated in the figure. In group 4, on the other hand, the probe was PI-27 with $M_I = 27\,000$ and the matrix M_B was changed as indicated. For comparison, the theoretical loss curve calculated with the Rouse/tube model (eq 2) is indicated with the heavy solid line.

We see that among the group 1 curves in the PB-03 matrix those of PI-27 and PI-86 agree fairly well with the Rouse curve, while with decreasing M_I (*e.g.*, PI-13

and PI-06) the loss curves appear to broaden considerably. This means that PB-03 acts as a solvent toward PI-27 and PI-86 in both the relaxation time and mode distribution. However, it should be noted that for these low-molecular-weight PI probes the separation between the normal- and segmental-mode peaks becomes narrow and therefore the overlapping of the low-f tail of the segmental mode process might cause the apparent broadening of the high-f tail of the normal mode peak. The subtraction of the contribution of the segmental mode peak by using the Havriliak–Negami equation is obviously unsatisfactory. At present, it is thus difficult to assess the broadening due to this effect.

In the group 2 curves for the PB-05 matrix, we see that the normal mode peaks of PI-48 and PI-27 in the high-f tail are slightly broader than but still close to the Rouse curve. Again with decreasing M_I (*e.g.*, PI-13 and PI-04) the normal mode peak appears to become broader, presumably partly because of the overlapping of the segmental mode peaks. We note that in the group 2, the matrix M_B is slightly larger than M_c of the PB melts and hence PB chains are in the entangled regime. Nevertheless the normal mode peak is still close to the Rouse curve. This implies that when $M_I \gg M_B$ the matrix chains behave as solvent and the M_I dependence as well as the distribution of relaxation times appears to conform to the Rouse theory. The loss curves for the blends with $M_I \ll M_B$ are shown in the group 3 curves. All the normal mode peaks are broader than the Rouse/tube theory curve. And in the group 4 curves we see that with increasing M_B the normal mode peak broadens from the loss curve of the Rouse model (for PB-03) to the bulk PI curve which has not yet been explained by any models.

Graessley's constraint release model predicts that if $M_g \gg M_m$, *i.e.*, $\tau_{d(g)} \gg \tau_{cr}$, the loss curve is of the Rouse-type, and with increasing M_m close to M_g, it becomes broader. This prediction qualitatively explains the observed broadening. However, the Graessley model further predicts that if $M_g \ll M_m$ (*i.e.*, $\tau_{d(g)} \ll \tau_{cr}$), the loss curve again resumes the Rouse model type, except the M_I dependence of the relaxation time. This prediction is contradictory to the observation.

Then an interesting question arises whether dilute blends with $M_I \gg M_B > M_e$ still satisfy the Rouse model or only dilute blends with ($M_I \gg$) $M_B < M_e$ (or $< M_c$ at most) do so? Although not yet confirmed by experiments, the implication is that the M dependence of τ is concerned: the former blends might behave like a dilute solution (as long as c_I does not exceed c_I^*). However, when the mode distribution is concerned, only the latter blends appear to satisfy the Rouse model.

As discussed above, the slope n of $\epsilon'' \propto f^{-n}$ in the high-f tail of the log ($\epsilon''/\epsilon_{max}''$) *versus* log($f/f_{max}$) curve is a measure of the broadening of the loss curve. In order to examine how the mode distribution changes as the M_I dependence of τ changes from the unentangled Rouse-like behavior to the entangled pure reptation behavior, we write in the values of n on a log τ_ζ *versus* log M_I graph, as shown in Figure 10. For the blends with $M_I < 5000$, the value of n is somewhat ambiguous because of the overlapping of the segmental mode. Otherwise along the Rouse line of M_I^2 dependence, the value n stays nearly at 0.5, indicating that the shape of the loss curves conforms to the Rouse theory. On the other hand, along the pure reptation line of M_I^3 dependence, the value n is around 0.3, indicating the significant broadening of the loss curves. In between where

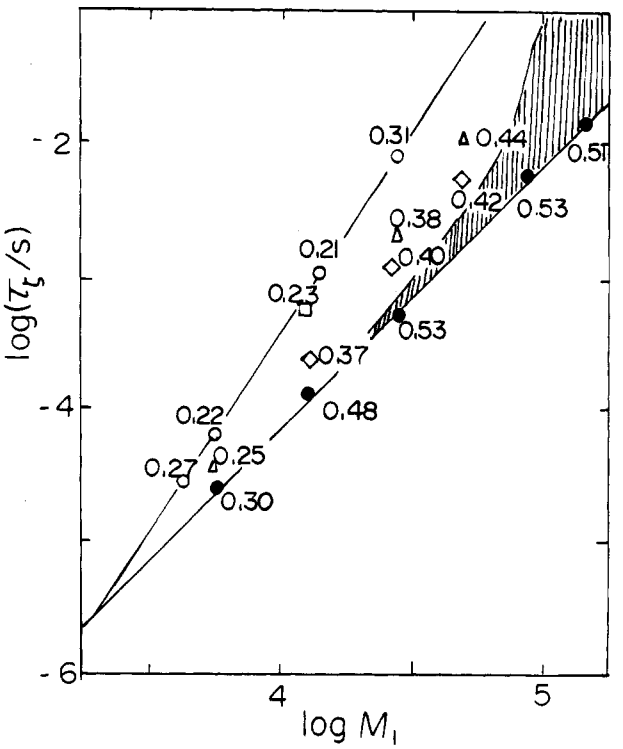

Figure 10. Slope n of $\epsilon'' \propto f^{-n}$ in the high-f tail plotted on a log τ_ζ *versus* log M_I graph for probe PI chains in different PB matrices.

log τ_ζ varies linearly with log M_I, as seen in Figure 5 and eqs 7 and 8, the value of n appears to increase from 0.37 to 0.44 as M_I/M_B is increased. Although not yet confirmed by experiments, we anticipate with further increase in M_I/M_B (or M_I) the value n might become 0.5, conforming to the Rouse theory in the hatched region of Figure 10. However, it is frustrating to see that in the region $M_e < M_I \ll M_B$ the pure reptation model well explains the M_I dependence of τ_ζ but apparently does not explain the distribution of relaxation times. The final conclusion remains to be seen in our future work.

Conclusion

1. The relaxation time τ of PI in a PB matrix was proportional to M_I^α with the index α increasing from 2.0 to 3.0 with increasing M_B from 2000 to 20 000 and up.

2. The index α for the blends at a constant ratio of M_I/M_B was higher than 3.0. When $M_I/M_B = 2-3$, the index α became 3.7, in agreement with the index observed for monodisperse PI melts.

3. The tube model combined with the theory of constraint release proposed by Graessley appears to consistently explain the observed behavior, excepting the relaxation mode distribution.

4. The relaxation mode distribution, *i.e.*, the shape of the loss curve, conforms to the Rouse theory when $M_I \gg M_B \leq M_e$, and the distribution becomes broader in the high-f tail with the decreasing ratio of M_I/M_B with $M_B \geq M_e$. However, for the case of $M_I/M_B < 1$ with $M_I > M_e$ the behavior is still ambiguous.

Acknowledgment. This work was partly supported by the Ministry of Education, Science, and Culture, Japan under a Grant-in-Aid for Scientific Research (04453106, 1992–1993).

References and Notes

(1) Stockmayer, W. H. *Pure Appl. Chem.* **1967**, *15*, 539.
(2) Adachi, K.; Kotaka, T. *Prog. Polym. Sci.* **1993**, *18*, 585.

(3) Kotaka, T.; Adachi, K. *Macromol. Chem., Macromol. Symp.* **1994**, *79*, 125; *Proc. IUPAC Microsymp., 33rd* **1993**.
(4) See, for example: Doi, M.; Edwards, S. F. *The Theory of Polymer Dynamics*: Clarendon Press; Oxford, U.K., 1986.
(5) Adachi, K.; Nishi, I.; Itoh, S.; Kotaka, T. *Macromolecules* **1990**, *23*, 2550. Adachi, K.; Itoh, S.; Nishi, I.; Kotaka, T. *Ibid.* **1990**, *23*, 2554.
(6) Adachi, K.; Nakamoto, T.; Kotaka, T. *Macromolecules* **1989**, *22*, 3111. Adachi, K.; Kotaka, T. *J. Non-Cryst. Solids* **1991**, *131–133*, 723.
(7) Watanabe, H.; Yamazaki, M.; Yoshida, H.; Adachi, K.; Kotaka, T. *Macromolecules* **1991**, *24*, 5365.
(8) Urakawa, O.; Adachi, K.; Kotaka, T. *Macromolecules* **1993**, *26*, 2036, 2042.
(9) Rouse, P. E. *J. Chem. Phys.* **1953**, *21*, 1272. Zimm, B. H. *Ibid.* **1956**, *24*, 269.
(10) De Gennes, P.-G. *J. Chem. Phys.* **1971**, *55*, 572.
(11) Doi, M.; Edwards, S. F. *J. Chem. Soc., Faraday Trans. 2* **1978**, *74*, 1789, 1802, 1818.
(12) Ferry, J. D. *Viscoelastic Properties of Polymers*, 3rd ed.; John Wiley: New York, 1980.
(13) Graessley, W. W. *Adv. Polym. Sci.* **1982**, *47*, 68.
(14) Pearson, D. S.; Fetters, L. J.; Graessley, W. W.; Ver Strate, G.; Von Meerwall, E. *Macromolecules* **1994**, *27*, 711.
(15) Doi, M. *J. Polym. Sci.* **1983**, *21*, 667; *J. Polym. Sci. Lett.* **1981**, *19*, 265.
(16) Klein, J. *Macromolecules* **1978**, *11*, 852.
(17) Watanabe, H.; Tirrell, M. *Macromolecules* **1989**, *22*, 927.
(18) Adachi, K.; Nakamoto, T.; Kotaka, T. *Macromolecules* **1989**, *22*, 3106.
(19) Clague, A. D.; Van Broekhaven, J. E. M.; Blawn, L. P. *Macromolecules* **1974**, *7*, 348.
(20) Williams, M. L.; Landel, R. F.; Ferry, J. D. *J. Am. Chem. Soc.* **1955**, *77*, 3701.
(21) Colby, R. H.; Fetters, L. J.; Graessley, W. W. *Macromolecules* **1987**, *20*, 2226.
(22) Flory, P. J. *J. Chem. Phys.* **1947**, *17*, 303. See also: Flory, P. J. *Principles of Polymer Chemistry*; Cornell University Press: Ithaca, NY, 1953.
(23) Verdier, R. H.; Stockmayer, W. H. *J. Chem. Phys.* **1962**, *36*, 227.
(24) Adachi, K.; Nishi, I.; Doi, H.; Kotaka, T. *Macromolecules* **1991**, *24*, 5843.

MA946159B